ECS Transactions, 98 (3) 99-105 (2020)
10.1149/09803.0099ecst ©The Electrochemical Society

Copper Oxide Passivation Effect on Electromigration of Plasma Etched Copper Lines

Jia Quan Su, Yue Kuo*

Thin Film Nano & Microelectronics Research Laboratory, Texas A&M University, College Station, Texas 77843, U.S.A. *yuekuo@tamu.edu

The degradation of the copper oxide passivated copper line prepared from a room temperature plasma-based etch process under the electromigration condition has been studied. The copper line surface was oxidized into the copper oxide layer in a parallel-plate plasma reactor operated under the plasma etching or reactive ion etching mode. The surface roughness of the oxide is contributed by the high ion bombardment energy. The lifetime of the sample was shortened by the addition of the oxide passivation layer. It was also decreased with the increase of the stress current density. The sample with the thin bulk copper layer is more resistant to the thermal stress than that with the thick bulk copper layer, which delayed the voids formation in the line breakage process.

Introduction

Copper (Cu) is the most common interconnect material in high density integrated circuits (ICs) and large-area thin film transistor (TFT) arrays due to its high conductivity, lack of hillocks formation, and high resistance to electromigration (EM) (1-3). Conventionally, the Damascene process is used in the fabrication of Cu interconnect lines (3-5). This method involves complicated process steps and environmentally unfriendly chemicals, e.g., strong oxidants, surfactants, and nano-particles. The end point is difficult to detect. Also, the dishing phenomenon is commonly observed in the wide Cu lines (6-8). Furthermore, this method is not applicable to the fabrication of large-area TFT arrays because the glass substrate is not flat.

Plasma etching is the most popular method in fabricating metal interconnect lines. The etched lines have well controlled profiles with tight critical dimensions (CDs) (9-13). However, the conventional plasma etching method cannot be applied to etch Cu because the reaction products, e.g., Cu halides, have low vapor pressures at room temperature (14). The high temperature or high energy beams are often applied to the substrate to remove reaction compounds (15,16). Kuo's group invented a novel plasma-based Cu etch process that was composed of two steps: first, a plasma chlorination or bromination reaction that converted the metallic Cu film into a porous Cu halide layer at a high rate; second, a dilute HCl solution dipping step that instantaneously dissolved the reaction product (17-19). This method has been successfully used in fabricating BiCMOS chips, 15" thin film transistor liquid crystal displays (TFT LCDs), and sub 0.3 μ patterns (20-23).

The electromigration (EM) method is commonly used to assess the reliability of the metal line. In the test, a high density current is passed through the line until it is broken (24). The EM line failure phenomena of the plasma-etched Cu line was first reported by Kuo's group (25). The Cu line width and length affected the EM failure time (26).

Since Cu cannot adhere well to the glass substrate, a barrier layer is required to improve the adhesion. Titanium-tungsten (TiW) and molybdenum (Mo) are popular barrier materials for this purpose. They can be easily etched with plasma processes (26-31). Separately, Cu is easily subjected to air oxidation under ambient atmosphere, which deteriorates the line quality. A capping layer can prevent this undesirable phenomena. Previously, there were studies on the capping layer effect on the EM lifetime of the Damascene prepared Cu lines (32,33), which is embedded in a trench structure surrounded by the dielectric material. However, the plasma etched Cu line is free-standing similar to the plasma etched aluminum line. Our recent studies showed that the TiW or Mo capping layer could protect the plasma-etched Cu lines from environmental attack but at the same time, reduced the lifetime (34-37).

Recently, copper oxide (CuO_x) has been proposed to be an effective passivation material for the plasma-etched Cu line (38,39). Advantages of this kind of passivation layer include: the simple fabrication method and the gettering of Cu atoms diffused from the bulk Cu layer (38). Since CuO_x only forms on the exposed Cu surface, it is a self-aligned passivation structure. In this study, authors investigated structures and wet etch of CuO_x passivation layers prepared under various plasma exposure conditions. The Cu film thickness on the EM lifetime is also investigated.

Experimental

Sample preparation

The TiW/Cu stack was sputter deposited in one pumpdown on a pre-cleaned Corning glass. The 10 nm thick TiW barrier film was sputter deposited at 80 W, 10 mTorr in Ar for 15 minutes. The Cu film was sputter deposited at 80W and 10 mTorr in Ar. The sample was defined into a 4-probe pattern using a mask aligner (Quintel Corporation Q-4000 Series) lithographically. The sample was dipped in a diluted HCl solution ($HCl:H_2O$ = 1:4 v/v) to remove the native oxides on the Cu surface. Then, the sample was exposed to the CF_4/HCl 5/20 sccm plasma at 70 mTorr, and 600 W for 2 minutes in a PlasmaTherm 700C system operated under the reactive ion etching (RIE) mode. After the Cu film was completely converted into $CuCl_x$, the sample was dipped in a diluted HCl solution ($HCl:H_2O$ = 1:8 v/v) for 1 minute to dissolve the chloride film. Subsequently, the TiW barrier layer was etched with the CF_4 plasma at 10 sccm, 60 mTorr, 600 W for 2 minutes. After the photoresist layer was stripped, the sample was oxidized in the O_2 plasma with the same PlasmaTherm 700C system operated at the plasma etching (PE) or the RIE mode. Separately, a control sample of TiW/Cu without the plasma oxidation step was prepared.

EM stress tests and sample analysis

For the reliability test, the sample was loaded on a probe station (Signatone S-1160) and stressed at a constant current density (J) between 4.05×10^5 and 1.16×10^6 Amp/cm^2. The current was supplied through an Agilent E3645A DC power supply controlled by a Labview program. The physical appearance of the Cu line was monitored through an optical microscope (Olympus BX41M). The scanning electron microscope (SEM) image of the sample was taken using a JEOL JSM-7500F. A 5 nm thick platinum/palladium (Pt/Pd 80/20 wt%) film was sputter deposited on the sample to prevent charge accumulation and image distortion during SEM. The resistance vs. stress time (R-t) curve was recorded.

Results and Discussions

Topography of CuO_x passivation layer

Figure 1 shows top views of CuO_x films prepared by plasma oxidation under (a) PE and (b) RIE modes, respectively. The CuO_x layer prepared under the PE mode has a smoother surface than that prepared under the RIE mode. Since the RIE oxidation condition involves the high ion bombard energy, the oxidation rates on the bulk grain and at grain boundaries are different, which causes the surface roughness (40).

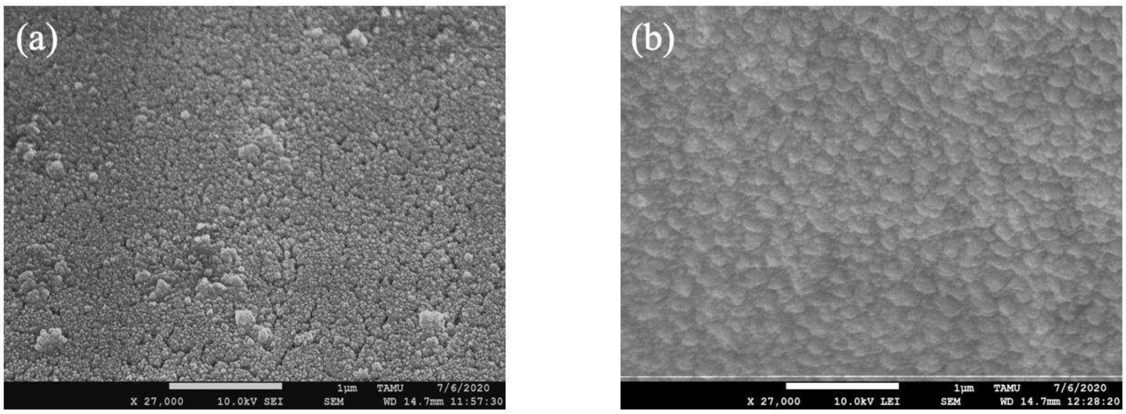

Figure 1. SEM top views of CuO_x passivation layer prepared by plasma oxidation under (a) PE mode at O_2 40 sccm, 200 mTorr, 300 W for 3 mins and (b) RIE mode at O_2 40 sccm, 100 mTorr, 300 W for 3 mins.

Figure 2 shows the high magnification (140 kX) top view of a CuO_x film formed from the RIE oxidation condition. The secondary electron (SE) image reveals the detailed granular structure of the film. Grains of various sizes are distributed on the CuO_x film.

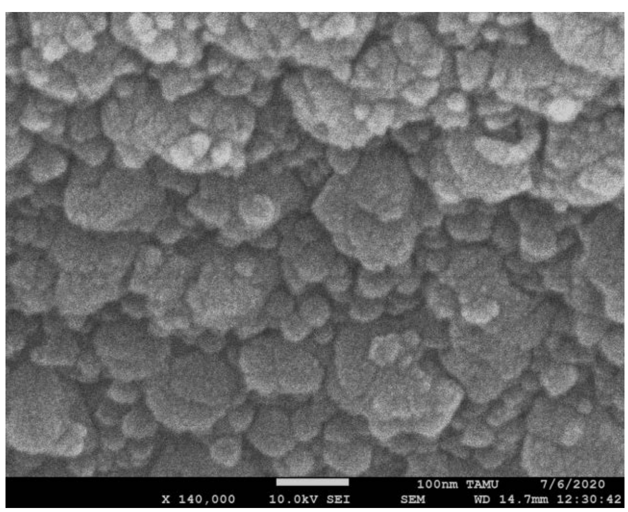

Figure 2. Top view of CuO_x prepared by plasma oxidation under RIE mode at O_2 40 sccm, 100 mTorr, 300 W for 3 mins.

Cu film thickness effect on EM lifetime

Figure 3 shows the EM lifetime vs. stress current density curves of CuO_x passivated samples of different Cu layer thicknesses. The lifetime of the sample decreases with the increase of the current density. The large stress current enhanced the voids formation and merging mechanism and hence accelerated the line breakage process (41). Fig. 3 also shows that under the same stress current condition, the CuO_x passivated line with a thin Cu bulk layer has a longer lifetime than that with a thick Cu layer. It was reported that during the EM stress, the temperature of the CuO_x passivated Cu line could reach around 1000ºC before it was broken (38). Thermal gradients could generate stress within the Cu line as shown in equation 1 (42). When the stress exceeds a critical value, void nucleation occurs (42). Thermal stress accelerates the formation and merging of voids.

$$\frac{d\sigma}{dt} = \frac{d}{dx}\left(\frac{DB\Omega}{k_B T}\left(\frac{d\sigma}{dx} + \frac{EZ^*e}{\Omega} - \frac{Q^*}{\Omega T}\frac{dT}{dx}\right)\right) \qquad [1]$$

where σ is the hydrostatic stress, t is the stress time, x is the line length assuming 1-dimensional structure, D is the effective atomic diffusivity, B is the effective bulk elastic modulus, Ω is the atomic volume, k_B is the Boltzmann constant, T is the temperature, E is the electric field, Z^* is the effective charge number, e is the fundamental electronic charge, and Q^* is the value of heat transport.

Lines with the thin bulk Cu film are experimentally shown to be more resistant to thermal stress (43). Therefore, lines with the thin bulk Cu film can afford higher thermal stress and inhibit void formation, which leads to a longer lifetime than that with the thick bulk Cu film. In addition, thermal stress could also contribute to the mechanical failure of the Cu line, known as thermal fatigue (43). It is reported that the yield stress would increase with the decrease of the film dimension, e.g., film thickness (44,45). Thus, the line with thick bulk Cu film would have a lower thermal yield stress and deformation could easily occur (43-45).

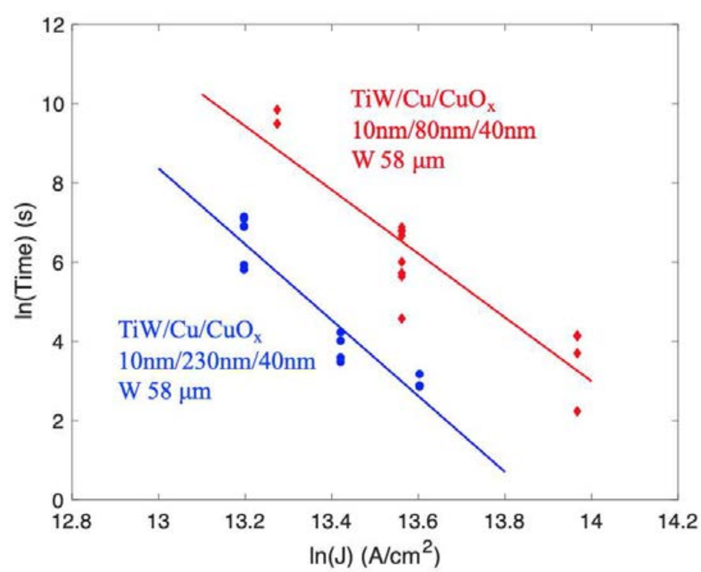

Figure 3. EM lifetime of CuO_x passivated Cu lines of different Cu film thickness under various stress current densities.

Wet etch of CuO_x passivation layer

Figure 4 shows top views of the photoresist patterned TiW/Cu/CuO_x sample before and after the removal of the CuO_x layer. The bulk Cu film was plasma oxidized under the condition of O_2 40 sccm, 200 mTorr at 600 W for 3 mins at PE mode. Fig. 4(a) is the sample partially covered with the AZ MiR 701 photoresist (PR) layer. Fig. 4(b) shows the sample after dipping in a dilute HCl solution (HCl:H_2O = 1:12 v/v) for 1 minute. About 130 nm thick of the CuO_x was removed in this step. As shown in eqn. 2, the standard electrode potential for Cu in a dilute acid without an oxidizing agent has a negative value, i.e., -0.34V. This means that this reaction would not occur spontaneously. On the other hand, the oxidized Cu, e.g., CuO, could be dissolved in a dilute HCl solution, as shown in eqn. 3 (46,47). Fig. 4(c) shows that after stripping off the PR, there is clear color difference between the CuO_x covered and uncovered Cu film. The CuO_x film has a darker appearance than the Cu film due to a difference of the refractive index.

$$Cu + 2H^+ \rightarrow Cu^{2+} + H_2 \qquad E^o = -0.34V \qquad [2]$$

$$CuO + 2HCl \rightarrow CuCl_2 + H_2O \qquad [3]$$

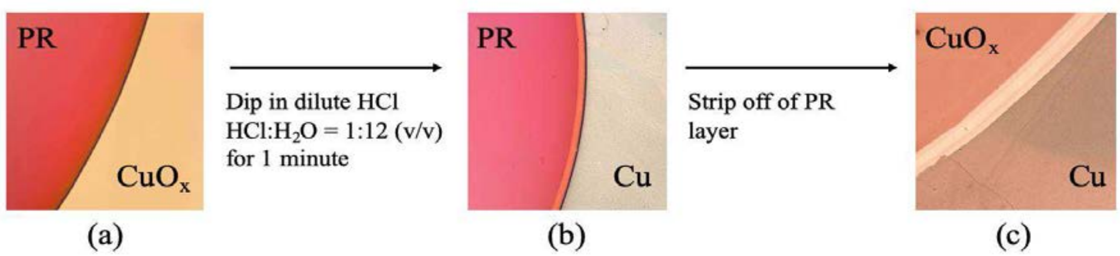

Figure 4. Top views of TiW/Cu/CuO_x sample (a) partially covered with photoresist, (b) removal of uncovered CuO_x film after dilute HCl solution dip, and (c) removal of photoresist layer.

Conclusion

The EM lifetime of the Cu line with CuO_x passivation layer was studied. CuO_x film could be formed on the Cu line in a plasma etcher under the PE or RIE condition. The CuO_x layer formed from the RIE oxidation condition had a rougher surface than that formed from the PE oxidation condition because of the strong ion bombardment energy. The CuO_x passivated Cu line with thin bulk Cu film had a longer EM lifetime than that with a thick bulk Cu film. The thin Cu film can withstand a higher thermal stress and has a higher yield stress than the latter. Therefore, voids are more difficult to form in the former to initiate the line breakage process than in the latter. The CuO_x passivation layer could be selectively removed from the Cu layer using a dilute HCl solution. In summary, the thickness of the bulk Cu layer is critical to the lifetime of the CuO_x passivated sample.

Acknowledgments

Authors acknowledge the support of this work by NSF CMMI project 1633580.

References

1. National Technology Roadmap for Semiconductors (NTRS), SIA, (1997).
2. Y. Kuo, *ECS Interface*, **22**(1), 55 (2013).
3. J. Proost, T. Hirato, T. Furuhara, K. Maex and J.-P. Celis, *J. Appl. Phys.*, **87**(6), 2792 (2000).
4. P. Wrschka, J. Hernandez, G. S. Oehrlein, J. A. Negrych, G. Haag, P. Rau and J. E. Currie, *J. Electrochem. Soc.*, **148**(6), G321 (2001).
5. C. S. Hau-Riege, S. P. Hau-Riege and A. P. Marathe, *J. Appl. Phys.*, **96**(10), 5792 (2004).
6. C. Yu, P. C. Fazan, V. K. Mathews and T. T. Doan, , *Appl. Phys. Lett.*, **61**(11), 1344 (1992).
7. M. Fayolle and F. Romagna, *Microelectron. Eng.*, **37**, 135 (1997).
8. R. Chang, Y. Cao and C. J. Spanos, *IEEE Trans. on Electron Dev.*, **51**(10), 1577 (2004).
9. P. M. Schaible, W. C. Metzger and J. P. Anderson, *J. Vac. Sci. Technol*, **15**(2), 334 (1978).
10. D. A. Danner, M. Dalvie and D. W. Hess, *J. Electrochem. Soc.*, **134**(3), 669 (1987).
11. Y. Kuo and J.R. Crowe, *J. Vac. Sci. Technol. A*, **8**(3), 1529 (1990).
12. P. E. Riley, *J. Electrochem. Soc.*, **140**(5), 1518 (1993).
13. D. J. Cooperberg, V. Vahedi and R. A. Gottscho, *J. Vac. Sci. Technol A*, **20**(5), 1536 (2002).
14. H. Miyazaki, K. Takeda, N. Sakuma, S. Kondo, Y. Homma and K. Hinode., *J. Vac. Sci. Technol B*, **15**(2), 237 (1997).
15. A. Bertz, T. Werner, N. Hille and T. Gessner, *Appl. Surf. Sci.*, **91**(1-4), 147 (1995).
16. C. Y. Nakakura and E. I. Altman, *Surf. Sci.*, **370**(1), 32 (1997).
17. Y. Kuo and S. Lee, *Japan J. of Appl. Phys.*, **39**(3A), L188 (2000).
18. S. Lee and Y. Kuo, *J. Electrochem. Soc.*, **148**(9), G524 (2001).
19. Y. Kuo and S. Lee, *Appl. Phys. Lett.*, **78**(7), 1002 (2001).
20. Y. Kuo and S. Lee, *Vacuum* **74(**3-4), 473 (2004).
21. Y. Kuo, Proc. 6th Intl. Conf. Reactive Plasmas & 23rd Symp. Plasma Processing, 29 (2006).
22. J. Yang, Y. Ahn, J. Bang, W. Ryu, J. Kim, J. Kang, M. S. Yang, I. Kang and I. Cung, *ECS Trans.*, **16**(9), 13 (2008).
23. Y. Kuo, J. Q. Su, M. Li and T. Yuan, XXXIV International Conference on Phenomena in Ionized Gases (XXXIV ICPIG), 10th International Conference on Reactive Plasmas (ICRP-10), Abst. OR19AM-B02, Sapporo, Hokkaido, Japan, July 14-19, (2019).
24. C. S. Hau-Riege, *Microelectron. Reliab.*, **44**(2), 195 (2004).
25. G. Liu and Y. Kuo, *J. Electrochem. Soc.*, **156**(7), H579 (2009).
26. M. Li and Y. Kuo, *ECS Trans.*, **86**(8), 41 (2018).
27. C. Ryu, H. Lee, K.-W. Kwon, A. LS. Loke and S. S. Wong, *Solid State Technol.*, **42**(4), 53 (1999).
28. S. Song, Y. Liu, D. Mao, H. Ling and M. Li, *Thin Solid Films*, **476**(1), 142 (2005).
29. J.-C. Chuang, S.-L. Tu and M.-C. Chen, *Thin Solid Films*, **346**(1-2), 299 (1999).
30. Y. Kuo, *J. Electrochem. Soc.*, **137**(6), 1907 (1990).
31. G. Liu and Y. Kuo, *J. Electrochem. Soc.*, **154**(7), H653 (2007).
32. M. C. Kang, Y. J. Kim and J. J. Kim, *Electrochem. Solid Lt.,* **12**(9), H340 (2009).

33. C-K. Hu, L. Gignac, E. Liniger, B. Herbst, D. L. Rath, S. T. Chen, S. Kaldor, A. Simon and W.-T. Tseng, *Appl. Phys. Lett.*, **83**(5), 869 (2003).
34. M. Li, J. Q. Su and Y. Kuo, *ECS Trans.*, **89**(3), 87 (2019).
35. J. Q. Su, M. Li and Y. Kuo, *ECS Trans.*, **90**(1), 65 (2019).
36. M. Li, J. Q. Su and Y. Kuo, *ECS Trans.*, **92**(5), 9 (2019).
37. J. Q. Su, M. Li, Y. Kuo and S. Hamaguchi, *ECS Trans.*, **92**(5), 39 (2019).
38. J. Q. Su and Y. Kuo, *ECS Trans.*, **97**(3), 51 (2020).
39. J. Q. Su and Y. Kuo, *MRS Adv.*, Accepted, July 2020.
40. A. U. Alam, M. M. R. Howlader and M. J. Deen, *J. Micromech. Microeng.*, **24**(3), 035010 (2014).
41. J. R. Black, *IEEE Trans.*, **16**(4), 338 (1969).
42. H. Zahedmanesh and K. Croes, *Microelectron. Reliab.*, **111**, 113769 (2020).
43. R. Mönig, Y.-B. Park and C. A. Volkert, *AIP Conf. Proc.*, **817**(1), 147 (2006).
44. C. V. Thompson, *J. Mater. Res.*, **8**(2), 237 (1993).
45. D. Y. W. Yu and F. Spaepen, *J. Appl. Phys.*, **95**(6), 2991 (2004).
46. J.-H. Chang, A. V. Ellis, C.-T. Yan and C.-H. Tung, *Sep. Purif. Technol.*, **68**(2), 216 (2009).
47. N. Habbache, N. Alane, S. Djerad and L. Tifouti, *Chem. Eng. J.*, **152**(2-3), 503 (2009).